Contribution from the Anorganisch-Chemisches Institut
der Universität Münster, D-4400 Münster, West Germany

Synthetic Route to $[Fe_6S_9(SR)_2]^{4-}$ Clusters (R = Alkyl). Their Spectroscopic and Magnetic Properties and the Solid-State Structures of $[Fe_6S_9(SCH_2Ph)_2]^{4-}$ and $[(Fe_6S_9(SMe)_2)_2Na_2]^{6-}$

HENRY STRASDEIT, BERNT KREBS, and GERALD HENKEL*

Received May 10, 1983

The hexanuclear iron–sulfide–thiolate complexes $[Fe_6S_9(SR)_2]^{4-}$ (R = Me, Et, CH_2Ph) have been prepared in methanolic solution by reaction of $Fe(SR)_3$ with Na_2S_2 and were isolated as black, air-sensitive crystals of $(Et_4N)_4[Fe_6S_9(SCH_2Ph)_2]\cdot H_2O$ (**1**), $(Et_4N)_4[Fe_6S_9(SEt)_2]$ (**2**), and $(Et_4N)_6[(Fe_6S_9(SMe)_2)_2Na_2]$ (**3**). The crystal and molecular structures of **1** and **3** have been determined from three-dimensional X-ray data. **1** crystallizes in the monoclinic space group $P2_1/c$ with a = 16.339 (3) Å, b = 19.535 (4) Å, c = 21.729 (4) Å, β = 106.56 (3)°, and Z = 4. Crystals of **3** were found to be monoclinic, space group $C2/m$, with a = 12.813 (13) Å, b = 28.626 (21) Å, c = 16.056 (17) Å, β = 129.06 (7)°, and Z = 2. The structures were solved by direct methods and refined to conventional R factors of 0.060 and 0.085, respectively. Crystals of **1** and **3** consist of discrete anions, cations, and, in the case of **1**, H_2O molecules. The $[Fe_6S_9(SCH_2Ph)_2]^{4-}$ anion possesses a nearly planar arrangement of the Fe atoms resulting from a coupling of six FeS_4 tetrahedra via common edges and corners. Structural characteristics of the $[Fe_6S_9]^{2-}$ core are Fe_3S_7 and Fe_4S_9 fragments, which represent subunits of the well-known cubane-type $[Fe_4S_4(SR)_4]^{2-,3-}$ clusters and the hypothetical $[Fe_8S_6(SR)_8]^{n-}$ cluster family with a cubic arrangement of Fe atoms, respectively. $[Fe_7MoS_6(SR)_7L_n]^{z-}$, a mixed-metal derivative, is supported as a structural and compositional model for the Mo–Fe center of nitrogenase. The Fe_3S_7 fragment is discussed in connection with the 3-Fe center of *Desulfovibrio gigas* ferredoxin II and beef heart aconitase. The structure of the novel $[(Fe_6S_9(SMe)_2)_2Na_2]^{6-}$ anion in crystals of **3** can be described in terms of two hexanuclear iron–sulfide–thiolate units that are connected by two sodium cations or, alternatively, in terms of four $[Fe_3NaS_4(SR)_6]^{5-}$ units condensed via adjacent sodium and sulfur corners. Temperature-dependent solid-state magnetic susceptibility data of **1** are qualitatively consistent with antiferromagnetic coupling of the Fe atoms within the cluster and a diamagnetic ground state below 20 K. The position of the isotropically shifted S–CH_2 ^1H NMR signal of **1** between 225 and 340 K was measured as well as the room-temperature ^1H NMR spectra of **2** and **3** and the infrared and electronic spectra of **1**, **2**, and **3**. For iron–sulfide–thiolate clusters an empirical correlation between the composition and the mean oxidation state of iron is given.

Introduction

The presence of non-heme iron–sulfur proteins in nearly all biological systems and their participation in many enzymatic processes were the main reasons for the preparation and study of iron–sulfide–thiolate complexes.[1] According to our present knowledge three structural types of biological significance, namely $[Fe_2S_2(SR)_4]^{2-}$ [2] and $[Fe_4S_4(SR)_4]^{2-,3-}$,[3,4] which are accepted to be representations of [2Fe-2S] and [4Fe-4S] protein sites, and $[Fe_3S(o\text{-}(SCH_2)_2C_6H_2R_2)_3]^{2-}$ with R = CH_3[5a] and R = H,[5b] whose Fe_3S_7 frame is in good agreement with the 3-Fe center of *Desulfovibrio gigas* ferredoxin II as derived from EXAFS data, have been synthesized and characterized by X-ray structural analyses. Recently, further polynuclear iron–sulfide–thiolate species, $[Fe_6S_9(SR)_2]^{4-}$ [6] and $[Fe_3S_4(SR)_4]^{3-}$,[6e,7] have been described. However, no protein active sites are known containing six iron atoms in a planar arrangement or a linear chain of three iron atoms as in the $[Fe_6S_9]^{2-}$ and $[Fe_3S_4]^{+}$ cores, respectively.

It has been shown by crystallographic and EXAFS studies that 3-Fe sites in proteins are probably of different types. The presence of a Fe_3S_3 ring with a twist-boat conformation and a mean Fe···Fe distance of 4.08 Å was established in ferredoxin I of *Azotobacter vinelandii* by X-ray diffraction.[8] Synthetic analogues for the oxidized and reduced forms,[9] respectively, of this 3-Fe site are the not yet prepared $[Fe_3S_3(SR)_6]^{3-,4-}$ complexes, which have only corner-sharing FeS_4 tetrahedra in contrast to all known synthetic iron–sulfide–thiolate species. On the basis of EXAFS data of *D. gigas* ferredoxin II and beef heart aconitase it has been suggested that these proteins may contain [3Fe-3S][10] or [3Fe-4S][11] centers with Fe···Fe distances of ca. 2.7 Å. Considering the chemical interconversions of 4-Fe and 3-Fe centers,[12] it is also conceivable that some 3-Fe sites may possess the $Fe_3(\mu_3\text{-}S)$ moiety of the cubane-like Fe_4S_4 clusters. Besides $[Fe_3S(o\text{-}(SCH_2)_2C_6H_2R_2)_3]^{2-}$ with R = CH_3[5a] and R = H[5b] the hypothetical $[Fe_3(\mu_3\text{-}S)(\mu\text{-}S)_3(SR)_3]^{n-}$ is a potential structural model for active sites of this kind.

(1) Holm, R. H. *Acc. Chem. Res.* **1977**, *10*, 427.
(2) Mayerle, J. J.; Denmark, S. E.; DePamphilis, B. V.; Ibers, J. A.; Holm, R. H. *J. Am. Chem. Soc.* **1975**, *97*, 1032.
(3) (a) Averill, B. A.; Herskovitz, T.; Holm, R. H.; Ibers, J. A. *J. Am. Chem. Soc.* **1973**, *95*, 3523. (b) Que, L., Jr.; Bobrik, M. A.; Ibers, J. A.; Holm, R. H. *Ibid.* **1974**, *96*, 4168. (c) Christou, G.; Garner, C. D. *J. Chem. Soc., Dalton Trans.* **1979**, 1093. (d) Hagen, K. S.; Reynolds, J. G.; Holm, R. H. *J. Am. Chem. Soc.* **1981**, *103*, 4054.
(4) (a) Cambray, J.; Lane, R. W.; Wedd, A. G.; Johnson, R. W.; Holm, R. H. *Inorg. Chem.* **1977**, *16*, 2565. (b) Laskowski, E. J.; Frankel, R. B.; Gillum, W. O.; Papaefthymiou, G. C.; Renaud, J.; Ibers, J. A.; Holm, R. H. *J. Am. Chem. Soc.* **1978**, *100*, 5322. (c) Berg, J. M.; Hodgson, K. O.; Holm, R. H. *Ibid.* **1979**, *101*, 4586.
(5) (a) Henkel, G.; Tremel, W.; Krebs, B. *Angew. Chem.* **1981**, *93*, 1072; *Angew Chem., Int. Ed. Engl.* **1981**, *20*, 1033. (b) Hagen, K. S.; Christou, G.; Holm, R. H. *Inorg. Chem.* **1983**, *22*, 309.
(6) (a) Christou, G.; Holm, R. H.; Sabat, M.; Ibers, J. A. *J. Am. Chem. Soc.* **1981**, *103*, 6269. (b) Henkel, G.; Strasdeit, H.; Krebs, B. *Angew. Chem.* **1982**, *94*, 204; *Angew. Chem., Suppl.* **1982**, 489; *Angew. Chem., Int. Ed. Engl.* **1982**, *21*, 201. (c) Henkel, G.; Strasdeit, H.; Krebs, B. *Proc. Int. Conf. Coord. Chem.* **1982**, *22*, 618 (Vol. 2). (d) Christou, G.; Sabat, M.; Ibers, J. A.; Holm, R. H. *Inorg. Chem.* **1982**, *21*, 3518. (e) Hagen, K. S.; Watson, A. D.; Holm, R. H. *J. Am. Chem. Soc.* **1983**, *105*, 3905.
(7) Hagen, K. S.; Holm, R. H. *J. Am. Chem. Soc.* **1982**, *104*, 5496.
(8) (a) Stout, C. D.; Ghosh, D.; Pattabhi, V.; Robbins, A. H. *J. Biol. Chem.* **1980**, *255*, 1797. (b) Ghosh, D.; Furey, W., Jr.; O'Donnell, S.; Stout, C. D. *Ibid.* **1981**, *256*, 4185. (c) Ghosh, D.; O'Donnell, S.; Furey, W., Jr.; Robbins, A. H.; Stout, C. D. *J. Mol. Biol.* **1982**, *158*, 73.
(9) Xavier, A. V.; Moura, J. J. G.; Moura, I. *Struct. Bonding (Berlin)* **1981**, *43*, 187.
(10) Antonio, M. R.; Averill, B. A.; Moura, I.; Moura, J. J. G.; Orme-Johnson, W. H.; Teo, B.-K.; Xavier, A. V. *J. Biol. Chem.* **1982**, *257*, 6646.
(11) Beinert, H.; Emptage, M. H.; Dreyer, J.-L.; Scott, R. A.; Hahn, J. E.; Hodgson, K. O.; Thomson, A. J. *Proc. Natl. Acad. Sci. U.S.A.* **1983**, *80*, 393.
(12) (a) Johnson, M. K.; Spiro, T. G.; Mortenson, L. E. *J. Biol. Chem.* **1982**, *257*, 2447. (b) Moura, J. J. G.; Moura, I.; Kent, T. A.; Lipscomb, J. D.; Huynh, B. H.; LeGall, J.; Xavier, A. V.; Münck, E. *Ibid.* **1982**, *257*, 6259. (c) Kent, T. A.; Dreyer, J.-L.; Kennedy, M. C.; Huynh, B. H.; Emptage, M. H.; Beinert, H.; Münck, E. *Proc. Natl. Acad. Sci. U.S.A.* **1982**, *79*, 1096.

0020-1669/84/1323-1816$01.50/0

It has been pointed out that iron complexes,[13] besides $Mo/S^{2-}/CN^-$ compounds,[14] may have been of importance during early phases of evolution. Due to the spontaneous self-assembly under appropriate conditions and the ubiquitous occurrence of some Fe/S core units in organisms, their possible role in chemical evolution has to be considered. Iron–sulfide units with inorganic ligands may have acted as catalysts in prebiotic syntheses, for example in the formation of peptides. We are concerned with the synthesis and characterization of new iron–thiolate and iron–sulfide–thiolate complexes mainly because of their biochemical and prebiotic relevance and their structural aspects. In the course of our studies on new reaction systems we succeeded in preparing $[Fe_6S_9(SCH_2Ph)_2]^{4-}$.[6b,c] In the present paper we report a general preparative method for $[Fe_6S_9(SR)_2]^{4-}$ clusters (R = alkyl)[15] and the properties of this new type of iron–sulfide–thiolate complexes. In addition the structures of the anions $[Fe_6S_9(SCH_2Ph)_2]^{4-}$ and $[(Fe_6S_9(SMe)_2)_2Na_2]^{6-}$ will be given in detail.

Experimental Section

Chemicals and Elemental Analyses. Anhydrous iron(III) chloride (>98%, Fluka), benzyl mercaptan (99%, Aldrich), ethyl mercaptan (98%, Merck), tetraphenylphosphonium bromide (96%, Merck), and tetraethylammonium halides (98%, Merck) were used as purchased. Sodium disulfide was prepared by reduction of sodium tetrasulfide in ethanolic solution according to a literature method.[16] Sodium methyl mercaptide was obtained as a white, moisture-sensitive powder by refluxing an excess of dimethyl disulfide (~99%, Ega) and small pieces of sodium metal in anhydrous tetrahydrofuran under nitrogen and subsequently evaporating to dryness. Tetrahydrofuran was dried over sodium wire. Methanol was distilled from $Mg(OMe)_2$ and degassed prior to use.

Elemental analyses were performed at the Institute of Organic Chemistry at the University of Münster and by the microanalytical laboratory Beller, Göttingen, West Germany.

Preparation of the Complexes. All manipulations were carried out under an atmosphere of pure nitrogen with use of gloveboxes and Schlenk-type apparatus.

A solution of sodium mercaptide was prepared by dissolving 2.07 g (90 mmol) of sodium metal and 90 mmol of the respective thiol in 100 mL of methanol. In the case of methyl mercaptide this solution was obtained by dissolving 6.31 g (90 mmol) of NaSMe. To the stirred solution was added 4.87 g (30 mmol) of $FeCl_3$ in 50 mL of methanol, resulting in a dark-green precipitate of ferric mercaptide. After ~$^1/_2$ h of stirring 3.30 g (30 mmol) of Na_2S_2 was added. Specifications concerning the further treatment of the individual reaction mixtures are given in the following.

$(Et_4N)_4[Fe_6S_9(SCH_2Ph)_2]\cdot H_2O$ (1). After addition of Na_2S_2, a green-brown solution formed, which later turned deep brown. After ~20 h of stirring at ambient temperature, the solution was filtered, and the black filtration residue was washed with small portions of methanol. Filtrate and extracts were combined, treated with 4.14 g (25 mmol) of Et_4NCl, and stored at 5 °C for 2 h. Subsequently, the cold solution was filtered to remove a small amount of dark precipitate. When the solution stood at 5 °C, black shiny crystals of **1** separated during the following days. After the solution stood at −25 °C for an additional day, the product was collected by filtration of the cold solution through a glass filter, washed with methanol and tetrahydrofuran to remove $(PhCH_2S)_2$, and dried in vacuo; yield 0.7–1.8 g (10–26%). Anal. Calcd for $C_{46}H_{96}Fe_6N_4OS_{11}$: C, 39.21; H, 6.87; Fe, 23.78; N, 3.98; S, 25.03. Found: C, 39.24; H, 6.84; Fe, 23.91; N, 3.59; S, 24.24.

$(Et_4N)_4[Fe_6S_9(SEt)_2]$ (2). Addition of Na_2S_2 resulted in the immediate formation of a deep brown solution, which was stirred overnight and filtered. Because of the good solubility of **2** in the reaction mixture only 10 mL of methanol was used to wash the filtration residue, and filtrate and extract were treated with 6.63 g (40 mmol) of Et_4NCl. After the solution stood at ambient temperature for ~1 h, a light precipitate was removed by filtration. When the solution stood at −25 °C for 2 days, small intergrown black crystals of **2** formed in the filtrate. The cold solution was filtered through a glass filter. The product was washed with tetrahydrofuran and dried in vacuo. A yield of 1.4 g (22%) was obtained. Anal. Calcd for $C_{36}H_{90}Fe_6N_4S_{11}$: C, 34.13; H, 7.16; Fe, 26.45; N, 4.42; S, 27.84. Found: C, 33.11; H, 7.03; Fe, 25.29; N, 4.19; S, 27.17; Na, 1.15.[17]

$(Et_4N)_6[(Fe_6S_9(SMe)_2)_2Na_2]$ (3). Upon addition of Na_2S_2, the $Fe(SMe)_3$ rapidly dissolved, resulting in a deep brown solution. After it was stirred overnight, the mixture was filtered and the residue extracted with small portions of methanol. The extracts were combined with the filtrate and treated with 5.25 g (25 mmol) of Et_4NBr. After $^1/_2$ h the solution was filtered to remove a small amount of light precipitate. Black crystals of **3** appeared in the filtrate a few hours later. After the mixture stood at ambient temperature for 3 days, the product was collected in a glass filter, washed with methanol, and dried in vacuo; yield 0.2–0.4 g (4–7%). Anal. Calcd for $C_{26}H_{66}Fe_6N_3NaS_{11}$: C, 27.60; H, 5.88; Fe, 29.61; N, 3.71; Na, 2.03; S, 31.17. Found: C, 27.52; H, 5.82; Fe, 29.66; N, 3.69; Na, 2.04; S, 30.99. A crystalline Ph_4P^+ salt was obtained in an analogous preparation, with use of Ph_4PBr instead of Et_4NBr. Well-shaped single crystals of **3** suitable for X-ray structural analysis were grown from a reaction mixture not moved during the addition of Et_4NBr and for the following 3 days.

X-ray Data Collection and Reduction. X-ray diffraction data were collected with an automated Syntex $P2_1$ four-circle diffractometer. A single crystal of **1** selected for data collection was sealed in a glass capillary under pure nitrogen, whereas the selected crystal of **3** was fixed with a trace of silicone grease at the top of a glass capillary and cooled by a stream of nitrogen with use of a modified Syntex LT-1 low-temperature device. The unit cell dimensions with standard deviations were derived from a least-squares fit from the scattering angles of 15 centered reflections in the range $20° < 2\theta < 30°$. The experimental data of the measurements are given in Table I together with relevant details of the structure refinements. The intensity profiles of the scans indicated stable crystal settings during data collection. While the intensities of a reference reflection remeasured every 99 scans exhibited only random fluctuations for **3**, a monotonic decrease as a function of exposure time was recorded for **1** consistent with a

Table I. Details of Data Collection and Structure Refinements for $(Et_4N)_4[Fe_6S_9(SCH_2Ph)_2]\cdot H_2O$ (1) and $(Et_4N)_6[(Fe_6S_9(SMe)_2)_2Na_2]$ (3)

	1	3
formula	$C_{46}H_{96}Fe_6N_4OS_{11}$	$C_{52}H_{132}Fe_{12}N_6Na_2S_{22}$
fw	1409.09	2263.22
a, Å	16.339 (3)	12.813 (13)
b, Å	19.535 (4)	28.626 (21)
c, Å	21.729 (4)	16.056 (17)
β, deg	106.56 (3)	129.06 (7)
V, Å^3	6647.8	4572.8
Z	4	2
d_{calcd}, g cm^{-3}	1.408	1.644
space group	$P2_1/c$	$C2/m$
temp, K	293	140
cryst dimens, mm	0.15 × 0.1 × 0.1	0.25 × 0.15 × 0.1
radiation (graphite monochromatized)	Mo Kα	Mo Kα
μ(Mo Kα), cm^{-1}	16.7	24.1
scan mode	θ–2θ	θ–2θ
scan speed (intensity dependent), deg min^{-1}	4–30	4–30
ratio bkgd/scan time	0.5	0.5
scan range, deg	2 + Kα splitting	3 + Kα splitting
(sin θ)/λ cutoff, Å^{-1}	0.57	0.57
index range	$+h,+k,\pm l$	$+h,+k,\pm l$
no. of (indep) reflcns measd	10 114	3420
reflcns used (rejection criterion)	6156 ($I > 2\sigma(I)$)	2355 ($I > 3\sigma(I)$)
no. of variables	608	209
R_1, R_2	0.060, 0.050	0.085, 0.088

(13) Beck, M. T. *Met. Ions Biol. Syst.* **1978**, *7* (Chapter 1).
(14) Müller, A.; Eltzner, W.; Bögge, H.; Jostes, R. *Angew. Chem.* **1982**, *94*, 783; *Angew. Chem., Suppl.* **1982**, 1643; *Angew. Chem., Int. Ed. Engl.* **1982**, *21*, 789.
(15) Other complexes with $[Fe_6S_9]^{2-}$ cores were prepared by procedures different from ours.[6a,d,e]
(16) Fehér, F.; Berthold, H. J. *Z. Anorg. Allg. Chem.* **1953**, *273*, 144.
(17) The product contains 2–3% NaCl.

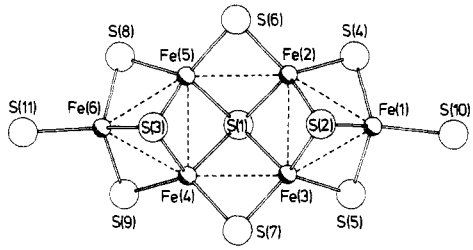

Figure 1. Projection of the Fe_6S_{11} frame with atomic labeling scheme for $(Et_4N)_4[Fe_6S_9(SCH_2Ph)_2]\cdot H_2O$.

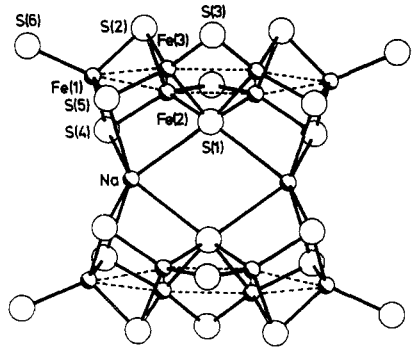

Figure 2. Projection of the $(Fe_6S_{11})_2Na_2$ frame with atomic labeling scheme for $(Et_4N)_6[(Fe_6S_9(SMe)_2)_2Na_2]$.

decay of 27% at the end of the measurement. The decomposition was accounted for by a scaling procedure. The intensities of both data sets were empirically corrected for absorption (ψ-scan method) and for Lorentz and polarization effects (Lp). The variance of I was calculated as $\sigma(I)^2 = S + (B_1 + B_2)(t_S/2t_B)^2$, where S, B_1, and B_2 are the scan and individual background counts, respectively, and t_S and t_B are their counting times.

Solutions and Refinements of the Structures. All calculations were performed with use of programs of the Syntex EXTL and SHELXTL program packages. In the case of **1** the space group could be unambiguously determined to be $P2_1/c$, whereas in the case of **3** the observed symmetry and the systematic absences were compatible with the monoclinic space groups $C2$, Cm, or $C2/m$. The centrosymmetric space group $C2/m$ was initially chosen from the distribution of the normalized structure factors and confirmed in the structure solution process. Starting points for the solution of both structures were provided by direct methods, resulting in the location of the iron and sulfur atoms. Repeated least-squares refinements followed by difference Fourier syntheses revealed the positions of all non-hydrogen atoms in the unit cells.

In the structure of **1** all atoms of the $[Fe_6S_9(SCH_2Ph)_2]^{4-}$ anion are symmetry independent, whereas the $[(Fe_6S_9(SMe)_2)_2Na_2]^{6-}$ anion in the structure of **3** has $2/m$ symmetry as imposed crystallographically. Due to a disorder of the tetraethylammonium ions and the thiolate methyl groups in the structure of **3**, no hydrogen contributions to the structure factors were taken into account. The methylene and phenyl hydrogen atoms in the structure of **1** were calculated in idealized positions as well as two of three methyl hydrogen atoms after choosing the best defined one from a difference Fourier synthesis. They were fixed in the subsequent refinement cycles at their initial positions with an isotropic temperature factor of $B = 10$ Å^2.

Final full-matrix least-squares refinement cycles with anisotropic temperature factors for all non-hydrogen atoms except O in the structure of **1** and all Fe, S, and Na atoms in the structure of **3** converged to $R_1 = \sum(||F_o| - |F_c||)/\sum|F_o| = 0.060$ and $R_2 = [\sum w(|F_o| - |F_c|)^2/\sum w|F_o|^2]^{1/2} = 0.050$ for **1** and $R_1 = 0.085$ and $R_2 = 0.088$ for **3**.

The quantity minimized was $\sum w(|F_o| - |F_c|)^2$, w being defined as $w = [\sigma^2(F_o) + (0.01F_o)^2]^{-1}$ with $\sigma(F_o) = \sigma(I)(Lp)^{-1}/2F_o$. Atomic scattering factors for spherical neutral free (all except H) or bonded (H) atoms as well as anomalous scattering contributions were taken from ref 18. The final positional parameters with standard deviations

(18) "International Tables for X-ray Crystallography"; Kynoch Press: Birmingham, England, 1974; Vol. IV.

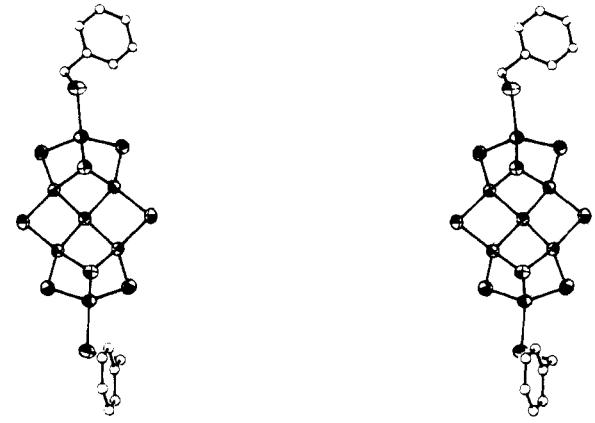

Figure 3. Stereoscopic view of the anion of $(Et_4N)_4[Fe_6S_9(SCH_2Ph)_2]\cdot H_2O$ with thermal ellipsoids of the Fe and S atoms (50% probability level, T = 293 K). The hydrogen atoms are omitted.

Scheme I

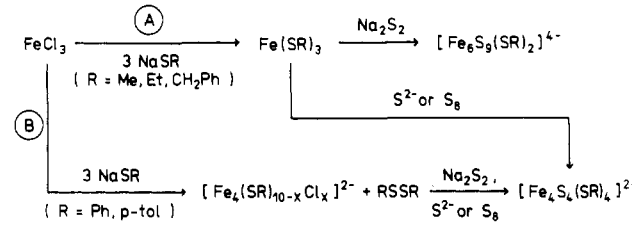

for **1** and **3** are summarized in Tables II and III. The labels of the Fe and S atoms are given in Figures 1 and 2; stereoscopic projections of the anions of **1** and **3**, with thermal ellipsoids (50% probability) of the Fe and S atoms, are displayed in Figures 3 and 4, respectively. In Tables IV and V listings of bond distances and valence angles within the anions of **1** and **3** are given together with selected nonbonded intramolecular separations.

Spectroscopic and Magnetic Susceptibility Measurements. The complexes studied are air-sensitive, especially in solution. Therefore, all measurements were performed under anaerobic conditions. Cary 17 and Perkin-Elmer 551S spectrophotometers were used for recording the electronic spectra. Infrared spectra were obtained on a Bruker IFS-114 FT-IR spectrometer at room temperature and 1 cm^{-1} resolution, using Nujol suspensions between polyethylene plates. The spectra of **1**–**3** in the range 700–100 cm^{-1} are shown in Figure S-1 of the supplementary material. The infrared absorptions in the region of Fe–S stretching vibrations (ca. 420–240 cm^{-1})[19] are given in Table VII. ^{1}H NMR spectra were recorded with a Bruker WM-300 spectrometer. The solvents acetonitrile-d_3 and Me_2SO-d_6 were ≥99% and 99.9%, respectively, deuterium enriched. Chemical shifts are given relative to Me_4Si as internal standard with downfield shifts being negative. Solid-state magnetic susceptibilities of **1** were determined in the temperature range 3.7–295 K with the Faraday–Curie method[20] and applied fields between 4×10^5 and 11×10^5 A m^{-1}.

Results and Discussion

Synthesis of $[Fe_6S_9(SR)_2]^{4-}$ Clusters. A summary of the reactions studied is given in Scheme I. $FeCl_3$ reacts with NaSR and Na_2S_2 in methanol, yielding different products depending on the nature of R. If R = methyl, ethyl or benzyl (A), the primary precipitate of ferric mercaptide dissolves on treatment with Na_2S_2 according to eq 1.

$$6Fe(SR)_3 + 6Na_2S_2 \rightarrow Na_4[Fe_6S_9(SR)_2] + 2NaSR + 3Na_2S + 7RSSR \quad (1)$$

The $[Fe_6S_9(SR)_2]^{4-}$ clusters can be separated from the deep

(19) Spiro, T. G.; Hare, J.; Yachandra, V.; Gewirth, A.; Johnson, M. K.; Remsen, E. In "Iron-Sulfur Proteins"; Spiro, T. G., Ed.; Wiley: New York, 1982; Chapter 11.

(20) Weiss, A.; Witte, H. "Magnetochemie"; Verlag Chemie: Weinheim, West Germany, 1973.

Table II. Positional Parameters for $(Et_4N)_4[Fe_6S_9(SCH_2Ph)_2]\cdot H_2O$

	x	y	z
Fe(1)	0.01234 (7)	0.83253 (6)	0.15659 (5)
Fe(2)	0.13515 (7)	0.74001 (6)	0.15417 (5)
Fe(3)	0.17272 (7)	0.87651 (6)	0.17036 (5)
Fe(4)	0.33651 (7)	0.85441 (6)	0.16498 (5)
Fe(5)	0.30391 (7)	0.71686 (6)	0.15286 (5)
Fe(6)	0.45932 (7)	0.76700 (6)	0.15259 (5)
S(1)	0.21338 (13)	0.80372 (10)	0.09931 (10)
S(2)	0.12793 (13)	0.80722 (11)	0.24036 (10)
S(3)	0.40428 (13)	0.76977 (11)	0.23609 (9)
S(4)	−0.00045 (14)	0.73718 (12)	0.09685 (11)
S(5)	0.05329 (14)	0.92637 (11)	0.11433 (11)
S(6)	0.21626 (14)	0.64669 (11)	0.18405 (11)
S(7)	0.28897 (14)	0.93668 (11)	0.21646 (11)
S(8)	0.38653 (14)	0.67951 (11)	0.09493 (10)
S(9)	0.42487 (14)	0.87029 (11)	0.10508 (10)
S(10)	−0.10940 (14)	0.86152 (12)	0.18196 (11)
S(11)	0.60356 (14)	0.75016 (13)	0.18621 (11)
C(1)	−0.1279 (6)	0.7868 (5)	0.2262 (4)
C(2)	−0.1127 (5)	0.8002 (4)	0.2967 (4)
C(3)	−0.0330 (6)	0.7994 (6)	0.3385 (5)
C(4)	−0.0210 (7)	0.8133 (7)	0.4031 (5)
C(5)	−0.0857 (6)	0.8252 (6)	0.4272 (5)
C(6)	−0.1648 (7)	0.8246 (7)	0.3858 (5)
C(7)	−0.1798 (6)	0.8113 (6)	0.3205 (5)
C(8)	0.6348 (6)	0.7728 (5)	0.1144 (4)
C(9)	0.6625 (5)	0.7140 (5)	0.0814 (4)
C(10)	0.7395 (5)	0.7169 (5)	0.0681 (4)
C(11)	0.7650 (6)	0.6623 (6)	0.0372 (4)
C(12)	0.7144 (6)	0.6065 (6)	0.0189 (5)
C(13)	0.6357 (7)	0.6043 (6)	0.0320 (5)
C(14)	0.6102 (6)	0.6594 (5)	0.0636 (5)
C(15)	0.4237 (6)	0.7245 (5)	0.4522 (4)
C(16)	0.4915 (6)	0.7264 (6)	0.4195 (5)
C(17)	0.2761 (5)	0.7317 (5)	0.4533 (4)
C(18)	0.1831 (6)	0.7405 (5)	0.4217 (4)
C(19)	0.3081 (6)	0.6866 (5)	0.3548 (4)
C(20)	0.3108 (7)	0.6138 (5)	0.3748 (5)
C(21)	0.3276 (6)	0.8070 (5)	0.3774 (4)
C(22)	0.3570 (7)	0.8664 (5)	0.4212 (5)
C(23)	0.4559 (6)	0.4017 (4)	0.2132 (4)
C(24)	0.4007 (6)	0.3551 (5)	0.1642 (5)
C(25)	0.4140 (7)	0.5071 (4)	0.1482 (4)
C(26)	0.4938 (8)	0.5108 (6)	0.1276 (6)
C(27)	0.3372 (6)	0.4780 (5)	0.2243 (5)
C(28)	0.3328 (7)	0.4465 (6)	0.2864 (6)
C(29)	0.4903 (6)	0.5131 (5)	0.2651 (4)
C(30)	0.4751 (6)	0.5868 (5)	0.2695 (5)
C(31)	0.2701 (7)	0.0917 (6)	0.1116 (5)
C(32)	0.2973 (8)	0.1637 (7)	0.1289 (6)
C(33)	0.2042 (6)	0.0059 (5)	0.0350 (5)
C(34)	0.1576 (7)	−0.0192 (5)	−0.0315 (6)
C(35)	0.2825 (6)	0.0983 (5)	−0.0017 (5)
C(36)	0.3643 (8)	0.0575 (6)	0.0107 (7)
C(37)	0.1471 (6)	0.1249 (5)	0.0176 (5)
C(38)	0.0835 (7)	0.1186 (6)	0.0541 (6)
C(39)	0.0881 (8)	0.9714 (5)	0.3003 (6)
C(40)	0.1467 (9)	0.9526 (7)	0.3658 (7)
C(41)	0.1165 (8)	1.0943 (6)	0.3118 (6)
C(42)	0.1770 (8)	1.0968 (6)	0.2721 (7)
C(43)	−0.0014 (9)	1.0480 (6)	0.3430 (7)
C(44)	−0.0745 (10)	0.9945 (7)	0.3337 (10)
C(45)	−0.0039 (7)	1.0495 (6)	0.2270 (6)
C(46)	−0.0481 (8)	1.1167 (7)	0.2124 (6)
N(1)	0.3346 (4)	0.7375 (3)	0.4098 (3)
N(2)	0.4249 (4)	0.4751 (3)	0.2122 (3)
N(3)	0.2253 (4)	0.0805 (4)	0.0393 (3)
N(4)	0.0501 (5)	1.0398 (3)	0.2969 (4)
O	0.1820 (10)	0.5633 (8)	0.0383 (8)

brown solutions by addition of tetraalkylammonium (Et_4N^+, $Me_3NCH_2Ph^+$) or Ph_4P^+ cations. In the case of R = benzyl the organic disulfide being formed in the redox process was isolated and, after two recrystallizations from methanol, identified by its melting point and IR spectrum. With aromatic mercaptides, such as R = phenyl, *p*-tolyl (B), $FeCl_3$ reacts to give yellow-brown solutions containing adamantane-like Fe(II) complexes.[3d] These solutions react immediately with Na_2S_2 to form $[Fe_4S_4(SR)_4]^{2-}$ complexes, which were isolated in good yields as Et_4N^+ salts and identified by their UV–visible spectra and elemental analyses. So the same products are isolated from the reaction with Na_2S_2 as with sulfide or elemental sulfur,[3a,c] and no direct preparation of $[Fe_6S_9(SR)_2]^{4-}$ clusters with arenethiolato ligands has been reported.[21]

Table III. Positional Parameters for $(Et_4N)_6[(Fe_6S_9(SMe)_2)_2Na_2]$

	population	x	y	z
Fe(1)	1	−0.01267 (20)	0.38473 (8)	0.26203 (16)
Fe(2)	1	−0.14244 (19)	0.38795 (7)	0.34488 (15)
Fe(3)	1	0.13353 (19)	0.38762 (7)	0.47841 (15)
S(1)	1	0.0	0.4334 (2)	0.5
S(2)	1	−0.0081 (4)	0.3292 (1)	0.3625 (3)
S(3)	1	0.2961 (4)	0.3636 (2)	0.6431 (3)
S(4)	1	−0.1951 (4)	0.4277 (1)	0.2040 (3)
S(5)	1	0.1743 (4)	0.4270 (1)	0.3819 (3)
S(6)	1	−0.0247 (5)	0.3518 (2)	0.1274 (4)
Na	0.5	−0.0070 (8)	0.5	0.3438 (6)
C(1a)	0.5	−0.125 (3)	0.390 (1)	0.019 (2)
C(1b)	0.5	0.104 (3)	0.391 (1)	0.142 (3)
C(2)	0.5	0.0	0.142 (1)	0.5
C(3)	0.5	−0.060 (4)	0.136 (1)	0.381 (3)
C(4)	0.5	0.038 (3)	0.197 (1)	0.635 (2)
C(5)	0.5	0.135 (3)	0.160 (1)	0.721 (2)
C(6)	0.5	−0.068 (3)	0.230 (1)	0.456 (2)
C(7)	0.5	−0.215 (3)	0.226 (1)	0.409 (3)
C(8)	0.5	0.172 (3)	0.197 (1)	0.565 (2)
C(9)	0.5	0.243 (3)	0.242 (1)	0.628 (3)
C(10)	0.5	0.180 (4)	0.200 (2)	0.100 (3)
C(11)	0.5	0.232 (3)	0.243 (1)	0.108 (3)
C(12)	0.5	0.0	0.143 (2)	0.0
C(13)	0.5	−0.050 (3)	0.137 (1)	0.063 (2)
C(14)	0.5	−0.062 (5)	0.238 (2)	−0.005 (5)
C(15)	0.5	−0.186 (8)	0.243 (4)	−0.137 (7)
C(16)	0.5	0.014 (5)	0.207 (2)	−0.103 (4)
C(17)	0.5	0.102 (5)	0.169 (2)	−0.111 (4)
C(18)	0.5	0.132 (3)	0.036 (1)	0.813 (2)
C(19)	0.5	0.201 (4)	0.019 (1)	0.765 (3)
C(20)	0.25	−0.012 (5)	−0.033 (2)	0.770 (4)
C(21)	0.5	−0.153 (2)	0.0	0.666 (2)
C(22)	0.25	0.061 (6)	0.029 (2)	0.902 (4)
C(23)	0.25	0.013 (5)	0.0	0.960 (3)
C(24)	0.5	0.176 (4)	−0.018 (1)	0.926 (3)
C(25)	0.25	0.348 (4)	0.0	1.031 (3)
C(26)	0.25	0.340 (4)	0.0	0.826 (3)
C(27)	0.25	−0.043 (5)	−0.031 (2)	0.690 (4)
C(28)	0.25	0.054 (5)	0.034 (2)	0.648 (4)
C(29)	0.25	0.008 (4)	0.0	0.541 (3)
N(1)	0.5	0.028 (2)	0.191 (1)	0.536 (1)
N(2)	0.5	0.023 (3)	0.198 (1)	−0.008 (2)
N(3)	0.25	0.097 (3)	0.0	0.857 (2)
N(4)	0.25	0.083 (3)	0.0	0.729 (2)

From the reaction mixtures that contained $[Fe_6S_9(SR)_2]^{4-}$ anions, no other iron–sulfide–thiolate species could be isolated. In particular, the formation of $[Fe_4S_4(SR)_4]^{2-}$ clusters is avoided. This may be due to the intermediate formation of iron–polysulfide complexes and to the fairly strong oxidizing effect of Na_2S_2. Though no polysulfide complexes were detectable during this specific reaction, their existence, on principle, has been proved by the synthesis of $[Fe_2S_2(S_5)_2]^{2-}$.[22] Na_2S_2 acts as an oxidant toward mercaptides, so that the amount of mercaptide is at least formally not sufficient for the assembly of $[Fe_4S_4(SR)_4]^{2-}$ clusters (cf. eq 1).

(21) $[Fe_6S_9(SPh)_2]^{4-}$ has been prepared in Me_2SO solution by ligand substitution from $[Fe_6S_9(S\text{-}t\text{-}Bu)_2]^{4-}$.[6a,d]

(22) (a) Coucouvanis, D.; Swenson, D.; Stremple, P.; Baenziger, N. C. *J. Am. Chem. Soc.* **1979**, *101*, 3392. (b) We found that $[Fe_2S_2(S_5)_2]^{2-}$ can easily be prepared by the reaction of $FeCl_2$, elemental sulfur, and CaH_2 at ca. 60 °C in dimethylformamide (unpublished work).

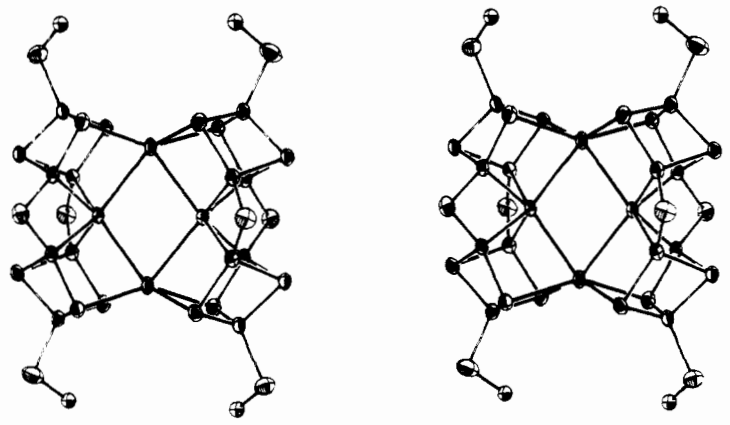

Figure 4. Stereoscopic view of the anion of $(Et_4N)_6[(Fe_6S_9(SMe)_2)_2Na_2]$ with thermal ellipsoids (50% probability level, T = 140 K).

Table IV. Interatomic Distances (Å) and Angles (deg) for $(Et_4N)_4[Fe_6S_9(SCH_2Ph)_2]\cdot H_2O$

		Fe-Fe	
Fe(1)-Fe(2)	2.712 (2)	Fe(3)-Fe(4)	2.746 (2)
Fe(1)-Fe(3)	2.692 (2)	Fe(4)-Fe(5)	2.737 (2)
Fe(2)-Fe(3)	2.736 (2)	Fe(4)-Fe(6)	2.706 (2)
Fe(2)-Fe(5)	2.802 (2)	Fe(5)-Fe(6)	2.723 (2)
		Fe-S	
Fe(1)-S(2)	2.273 (2)	Fe(4)-S(1)	2.330 (2)
Fe(1)-S(4)	2.246 (3)	Fe(4)-S(3)	2.318 (2)
Fe(1)-S(5)	2.236 (3)	Fe(4)-S(7)	2.221 (3)
Fe(1)-S(10)	2.282 (3)	Fe(4)-S(9)	2.224 (3)
mean	2.259	mean	2.273
Fe(2)-S(1)	2.339 (2)	Fe(5)-S(1)	2.332 (2)
Fe(2)-S(2)	2.318 (2)	Fe(5)-S(3)	2.310 (2)
Fe(2)-S(6)	2.238 (2)	Fe(5)-S(6)	2.223 (3)
Fe(2)-S(4)	2.211 (3)	Fe(5)-S(8)	2.215 (3)
mean	2.277	mean	2.270
Fe(3)-S(1)	2.331 (2)	Fe(6)-S(3)	2.244 (2)
Fe(3)-S(2)	2.306 (2)	Fe(6)-S(8)	2.249 (2)
Fe(3)-S(7)	2.215 (3)	Fe(6)-S(9)	2.263 (2)
Fe(3)-S(5)	2.210 (3)	Fe(6)-S(11)	2.284 (3)
mean	2.266	mean	2.260
		S···S	
S(1)···S(2)	3.713 (3)	S(1)···S(4)	3.714 (3)
S(1)···S(3)	3.704 (3)	S(1)···S(5)	3.630 (3)
S(1)···S(6)	3.571 (3)	S(1)···S(8)	3.749 (3)
S(1)···S(7)	3.600 (3)	S(1)···S(9)	3.661 (3)
S(2)···S(1)	3.713 (3)	S(3)···S(1)	3.704 (3)
S(2)···S(6)	3.798 (3)	S(3)···S(6)	3.810 (3)
S(2)···S(7)	3.790 (3)	S(3)···S(7)	3.729 (3)
S(2)···S(4)	3.503 (3)	S(3)···S(8)	3.478 (3)
S(2)···S(5)	3.536 (3)	S(3)···S(9)	3.552 (3)
S(2)···S(10)	3.869 (3)	S(3)···S(11)	3.733 (3)
S(4)···S(1)	3.714 (3)	S(5)···S(1)	3.630 (3)
S(4)···S(2)	3.503 (3)	S(5)···S(2)	3.536 (3)
S(4)···S(6)	3.928 (3)	S(5)···S(7)	3.863 (3)
S(4)···S(5)	3.793 (3)	S(5)···S(4)	3.793 (3)
S(4)···S(10)	3.790 (3)	S(5)···S(10)	3.613 (3)
S(8)···S(1)	3.749 (3)	S(9)···S(1)	3.661 (3)
S(8)···S(3)	3.478 (3)	S(9)···S(3)	3.552 (3)
S(8)···S(6)	3.869 (3)	S(9)···S(7)	3.941 (3)
S(8)···S(9)	3.775 (3)	S(9)···S(8)	3.775 (3)
S(8)···S(11)	3.795 (3)	S(9)···S(11)	3.769 (3)
S(6)···S(1)	3.571 (3)	S(7)···S(1)	3.600 (3)
S(6)···S(2)	3.798 (3)	S(7)···S(2)	3.790 (3)
S(6)···S(3)	3.810 (3)	S(7)···S(3)	3.729 (3)
S(6)···S(4)	3.928 (3)	S(7)···S(5)	3.863 (3)
S(6)···S(8)	3.869 (3)	S(7)···S(9)	3.941 (3)
S(10)··S(2)	3.869 (3)	S(11)··S(3)	3.733 (3)
S(10)··S(4)	3.790 (3)	S(11)··S(8)	3.795 (3)
S(10)··S(5)	3.613 (3)	S(11)··S(9)	3.769 (3)
		S-Fe-S	
S(2)-Fe(1)-S(4)	101.64 (9)	S(3)-Fe(6)-S(8)	101.46 (9)
S(2)-Fe(1)-S(5)	103.27 (9)	S(3)-Fe(6)-S(9)	104.03 (9)
S(2)-Fe(1)-S(10)	116.30 (9)	S(3)-Fe(6)-S(11)	111.09 (9)
S(4)-Fe(1)-S(5)	115.59 (10)	S(8)-Fe(6)-S(9)	113.60 (9)
S(4)-Fe(1)-S(10)	113.68 (10)	S(8)-Fe(6)-S(11)	113.73 (9)
S(5)-Fe(1)-S(10)	106.21 (10)	S(9)-Fe(6)-S(11)	111.97 (9)
S(1)-Fe(2)-S(2)	105.75 (9)	S(1)-Fe(4)-S(3)	105.68 (8)
S(1)-Fe(2)-S(6)	102.52 (9)	S(1)-Fe(4)-S(7)	104.54 (9)
S(1)-Fe(2)-S(4)	109.36 (9)	S(1)-Fe(4)-S(9)	106.98 (9)
S(2)-Fe(2)-S(6)	112.91 (9)	S(3)-Fe(4)-S(7)	110.47 (9)
S(2)-Fe(2)-S(4)	101.28 (9)	S(3)-Fe(4)-S(9)	102.89 (9)
S(6)-Fe(2)-S(4)	123.94 (10)	S(7)-Fe(4)-S(9)	124.92 (10)
S(1)-Fe(3)-S(2)	106.44 (9)	S(1)-Fe(5)-S(3)	105.83 (8)
S(1)-Fe(3)-S(7)	104.69 (9)	S(1)-Fe(5)-S(6)	103.22 (9)
S(1)-Fe(3)-S(5)	106.11 (9)	S(1)-Fe(5)-S(8)	111.02 (9)
S(2)-Fe(3)-S(7)	113.93 (9)	S(3)-Fe(5)-S(6)	114.36 (9)
S(2)-Fe(3)-S(5)	103.05 (9)	S(3)-Fe(5)-S(8)	100.40 (9)
S(7)-Fe(3)-S(5)	121.59 (10)	S(6)-Fe(5)-S(8)	121.32 (10)
		Fe-S-Fe	
Fe(2)-S(1)-Fe(3)	71.74 (7)	Fe(2)-S(6)-Fe(5)	77.82 (8)
Fe(2)-S(1)-Fe(4)	114.57 (9)	Fe(3)-S(7)-Fe(4)	76.48 (8)
Fe(2)-S(1)-Fe(5)	73.71 (7)	Fe(1)-S(4)-Fe(2)	74.96 (8)
Fe(3)-S(1)-Fe(4)	72.20 (7)	Fe(1)-S(5)-Fe(3)	74.52 (8)
Fe(3)-S(1)-Fe(5)	111.92 (9)	Fe(5)-S(8)-Fe(6)	75.18 (8)
Fe(4)-S(1)-Fe(5)	71.91 (7)	Fe(4)-S(9)-Fe(6)	74.17 (8)
Fe(1)-S(2)-Fe(2)	72.43 (7)		
Fe(1)-S(2)-Fe(3)	72.03 (7)		
Fe(2)-S(2)-Fe(3)	72.58 (7)		
Fe(4)-S(3)-Fe(5)	72.52 (7)		
Fe(4)-S(3)-Fe(6)	72.76 (7)		
Fe(5)-S(3)-Fe(6)	73.44 (7)		

Holm and co-workers reported the formation of $[Fe_6S_9(S\text{-}t\text{-}Bu)_2]^{4-}$ in a methanolic $FeCl_3/Li(S\text{-}t\text{-}Bu)/LiOMe/Li_2S$ reaction system and suggested that the suppression of $[Fe_4S_4(SR)_4]^{2-}$ cluster formation under these special conditions is possibly effected by iron–methylate intermediates.[6d] In this respect the recently prepared polynuclear iron complexes $[Fe_3(S_2P(p\text{-}tol)_2)_4(\mu\text{-}OMe)_2(MeOH)_2]$ and $[Fe_5(S_2P(p\text{-}tol)_2)_4(\mu_3\text{-}OMe)_2(\mu\text{-}OMe)_6]^-$ containing both dithiophosphinato and bridging methylato ligands are of interest. They can be obtained from simple reagents in methanolic solution and possess a linear Fe_3 and a spirocyclopentane-like Fe_5 framework, respectively.[23]

Description and Discussion of the Structures. The crystal structures of the mixed-valence compounds $(Et_4N)_4[Fe_6S_9(SCH_2Ph)_2]\cdot H_2O$ (**1**) and $(Et_4N)_6[(Fe_6S_9(SMe)_2)_2Na_2]$ (**3**) consist of discrete anions, cations, and, in the case of **1**, H_2O molecules. Characteristic features of both compounds are Fe_6S_9 fragments, which occur in the $[Fe_6S_9(SCH_2Ph)_2]^{4-}$ anion of **1** as monomeric cores and in the $[(Fe_6S_9(SMe)_2)_2Na_2]^{6-}$

(23) Henkel, G.; Bönnighausen, U.; Greiwe, K.; Krebs, B. *Proc. Int. Conf. Coord. Chem.* **1982**, *22*, 619 (Vol. 2).

Table V. Interatomic Distances (Å) and Angles (deg) for $(Et_4N)_6[(Fe_6S_9(SMe)_2)_2Na_2]$

		Fe–Fe	
Fe(1)–Fe(2)	2.707 (4)	Fe(2)–Fe(3)	2.767 (3)
Fe(1)–Fe(3)	2.718 (3)	Fe(2)–Fe(3)[a]	2.747 (4)
		Fe···Fe	
Fe(2)···Fe(2)[a]	3.902 (3)	Fe(3)···Fe(3)[a]	3.896 (4)
		Fe–S	
Fe(1)–S(2)	2.239 (5)	Fe(1)–S(5)	2.257 (5)
Fe(1)–S(4)	2.259 (6)	Fe(1)–S(6)	2.273 (6)
		mean	2.257
Fe(2)–S(1)	2.345 (3)	Fe(3)–S(1)	2.348 (4)
Fe(2)–S(2)	2.293 (5)	Fe(3)–S(2)	2.301 (4)
Fe(2)–S(4)	2.224 (4)	Fe(3)–S(5)	2.229 (5)
Fe(2)–S(3)[a]	2.209 (6)	Fe(3)–S(3)	2.205 (4)
mean	2.268	mean	2.271
		Na–S	
Na–S(1)	3.106 (8) (2×)	Na–S(5)	2.891 (9) (2×)
Na–S(4)	2.883 (7) (2×)		
		S···S	
S(1)···S(2)	3.674 (6) (2×)	S(1)···S(4)	3.727 (3) (2×)
S(1)···S(3)	3.561 (6) (2×)	S(1)···S(5)	3.737 (5) (2×)
S(2)···S(1)	3.674 (6)	S(2)···S(4)	3.534 (5)
S(2)···S(3)	3.786 (6)	S(2)···S(5)	3.532 (6)
S(2)···S(3)[a]	3.765 (8)	S(2)···S(6)	3.701 (7)
S(3)···S(1)	3.561 (6)	S(3)···S(5)	3.882 (6)
S(3)···S(2)	3.786 (6)	S(3)···S(4)[a]	3.882 (7)
S(3)···S(2)[a]	3.766 (8)		
S(4)···S(1)	3.727 (3)	S(5)···S(1)	3.737 (5)
S(4)···S(2)	3.534 (5)	S(5)···S(2)	3.532 (6)
S(4)···S(3)[a]	3.882 (7)	S(5)···S(3)	3.882 (6)
S(4)···S(5)	3.678 (7)	S(5)···S(4)	3.678 (7)
S(4)···S(6)	3.794 (8)	S(5)···S(6)	3.834 (6)
S(6)···S(2)	3.701 (7)	S(6)···S(5)	3.834 (6)
S(6)···S(4)	3.794 (8)		
		S–Fe–S	
S(2)–Fe(1)–S(4)	103.6 (2)	S(4)–Fe(1)–S(5)	109.1 (2)
S(2)–Fe(1)–S(5)	103.6 (2)	S(4)–Fe(1)–S(6)	113.7 (2)
S(2)–Fe(1)–S(6)	110.2 (2)	S(5)–Fe(1)–S(6)	115.6 (2)
S(1)–Fe(2)–S(2)	104.8 (2)	S(1)–Fe(3)–S(2)	104.4 (2)
S(1)–Fe(2)–S(4)	109.3 (2)	S(1)–Fe(3)–S(5)	109.4 (2)
S(1)–Fe(2)–S(3)[a]	102.9 (2)	S(1)–Fe(3)–S(3)	102.9 (2)
S(2)–Fe(2)–S(4)	103.0 (2)	S(2)–Fe(3)–S(5)	102.5 (2)
S(2)–Fe(2)–S(3)[a]	113.5 (2)	S(2)–Fe(3)–S(3)	114.3 (2)
S(4)–Fe(2)–S(3)[a]	122.3 (2)	S(5)–Fe(3)–S(3)	122.2 (2)
		S–Na–S	
S(1)–Na–S(1)[b]	75.7 (2)	S(4)–Na–S(4)[b]	91.7 (3)
S(1)–Na–S(4)	76.9 (2) (2×)	S(4)–Na–S(5)	79.2 (2) (2×)
S(1)–Na–S(4)[b]	130.8 (3) (2×)	S(4)–Na–S(5)[b]	148.2 (3) (2×)
S(1)–Na–S(5)	77.0 (2) (2×)	S(5)–Na–S(5)[b]	92.7 (3)
S(1)–Na–S(5)[b]	131.5 (3) (2×)		
		M–S–M	
Na–S(1)–Na[a]	104.3 (2)	Fe(2)–S(1)–Fe(2)[a]	112.6 (1)
Na–S(1)–Fe(2)	82.9 (2) (2×)		
Na–S(1)–Fe(2)[a]	143.7 (2) (2×)	Fe(2)–S(1)–Fe(3)	71.7 (1) (2×)
Na–S(1)–Fe(3)	82.9 (2) (2×)		
Na–S(1)–Fe(3)[a]	144.0 (2) (2×)	Fe(2)–S(1)–Fe(3)[a]	72.2 (1) (2×)
		Fe(3)–S(1)–Fe(3)[a]	112.1 (1)
Fe(1)–S(2)–Fe(2)	73.4 (2)	Fe(2)–S(2)–Fe(3)	73.5 (2)
Fe(1)–S(2)–Fe(3)	73.5 (2)		
Fe(1)–S(4)–Na	86.0 (2)	Fe(1)–S(5)–Na	85.8 (2)
Fe(1)–S(4)–Fe(2)	74.3 (2)	Fe(1)–S(5)–Fe(3)	74.6 (2)
Na–S(4)–Fe(2)	90.4 (2)	Na–S(5)–Fe(3)	90.2 (2)
Fe(3)–S(3)–Fe(2)[a]	77.6 (2)		

[a] Symmetry transformation: $-x, y, 1-z$. [b] Symmetry transformation: $x, 1-y, z$.

anions of **3** as subunits of cubane-like heterometallic Fe–Na–S clusters connected via adjacent corners and bridged by μ-S atoms to give $[(Fe_{3/1}Na_{1/2}S_{3/1}S_{1/2})S_{2/2}]_4^{2-}$ (**4**) cores.

The Fe_6S_{11} framework of **1** (**5**) and those of $[Fe_6S_9(S\text{-}t\text{-}Bu)_2]^{4-}$ (**6**)[6d] and $[Fe_6S_9(SEt)_2]^{4-}$ (**7**)[6e] show extensive structural similarities to the related subunit of **3**, though there are some differences as a consequence of the additional metal centers in the mixed iron–sodium–sulfur cluster of **3**. As principal features of the $[Fe_6S_9(SR)_2]^{4-}$ structural unit have been described earlier,[6] the following discussion is focused on more general questions concerning structural analogies to known iron–sulfur clusters as well as new structural principles and conclusions derived thereof.

The structure of **5** can be described in terms of six FeS_4 tetrahedra. They are coupled via common edges and corners to give a planar metal arrangement that consists of two triangles participating in a central Fe_4 square. The S atoms of **5** are involved in four distinct coordination modes reflecting the number of FeS_4 tetrahedra they are belonging to. These numbers are 1 (for the terminally bound thiolato S atoms S(10) and S(11)), 2 (for the μ-S atoms S(4)–S(9)), 3 (for the μ_3-S atoms S(2) and S(3)), and 4 (for the μ_4-S atom S(1)), respectively. According to the symmetry of **5**, which is very close to C_{2v}, the μ-S atoms divide into two sets (designated as S^a and S^b), depending on whether the bridged iron atoms are related by symmetry (S(6), S(7)) or not (S(4), S(5), S(8), S(9)). Under C_{2v} core symmetry the four (μ_4-S)–Fe bonds as well as the (μ-S)–Fe bonds of S(6) and S(7) are equivalent. As S(2) and S(3) as well as S(4), S(5), S(8), and S(9) connect nonequivalent Fe atoms, a distinction between bonds formed to one of the four central or to one of the two outer metal atoms (designated as Fe^a and Fe^b, respectively) should be made.

Though the mean Fe–S bond lengths decrease in the series Fe^a–(μ_4-S) (2.333 Å), Fe^a–(μ_3-S) (2.313 Å), and Fe^a–(μ-S) (2.224 Å), an unexpected trend in the Fe^b–(μ_3-S) and Fe^b–(μ-S) bonds is obvious, showing the former (2.259 Å) being shortened and the latter (2.249 Å) being elongated compared to the corresponding bonds involving Fe^a. As the mean oxidation state of iron in **1** is +2.67, a condition that can formally be satisfied for Fe^b and Fe^a within the limits +2, +3 and +3, +2.5, respectively, no conclusions concerning charge distributions within the Fe_6 frame can be drawn from arguments considering only bond lengths between iron and inorganic sulfur. As the mean Fe–S bond length of the FeS_4 tetrahedron should be related to the oxidation state of iron,[24] it follows that the central iron atoms (mean Fe^a–S = 2.272 Å) are formally in lower oxidation states than the outer ones (mean Fe^b–S = 2.260 Å). This interpretation is in agreement with ^{57}Fe Mössbauer results[6b] and is further supported by comparison of the mean Fe–S distances in **1** with reference values for $Fe^{2.5+}$ found to be 2.278 Å in $[Fe_4S_4(SCH_2Ph)_4]^{2-}$ and 2.281 Å in $[Fe_4S_4(SPh)_4]^{2-}$ and for Fe^{3+} found to be 2.257 Å in $[Fe_2S_2(S_2\text{-}o\text{-}xyl)_2]^{2-}$ and $[Fe_2S_2(S\text{-}p\text{-}tol)_4]^{2-}$, respectively.[25]

The most striking structural characteristics of **5** are Fe_3S_7 and Fe_4S_9 fragments (e.g. Fe(1), Fe(2), Fe(3), S(1), S(2), S(4), S(5), S(6), S(7), S(10) and Fe(2), Fe(3), Fe(4), Fe(5), S(1), S(2), S(3), S(4), S(5), S(6), S(7), S(8), S(9) (see Figure 1)), which represent subunits of two basic metal–sulfur cage structures, namely the cubane-type $[M_4S_4(SR)_4]^{n-}$ cluster with tetrahedral metal and inorganic sulfur arrangement and the metal cubane-type $[M_8S_6(SR)_8]^{n-}$ cluster with metal and inorganic sulfur atoms arranged in a cubic and octahedral manner, respectively.

$[Fe_4S_4(SR)_4]^{2-}$ cubane clusters are now well-known due to

(24) Hoggins, J. T.; Steinfink, H. *Inorg. Chem.* **1976**, *15*, 1682.
(25) Berg, J. M.; Holm, R. H. In "Iron-Sulfur Proteins"; Spiro, T. G., Ed.; Wiley: New York, 1982; Chapter 1.

the extensive studies of Holm and collaborators,[25] whereas derivatives containing the Fe_3S_7 frame of **1**, **3**, **6**, and **7** could be prepared only recently.[5,26] Trinuclear iron–sulfide–thiolate species are of special interest due to the more general significance of 3-Fe sites in iron–sulfur proteins. Though an X-ray structure determination shows the 3-Fe center of *A. vinelandii* ferredoxin I (Av fd I) to consist of a six-membered Fe_3S_3 ring[8] with Fe···Fe separations (mean value 4.08 Å) roughly as large as those between opposite atoms in the Fe_4 square of **5** (mean value 3.899 Å) (and thus much larger than those between direct neighbors), EXAFS investigations of *D. gigas* ferredoxin II (Dg fd II)[10] and beef heart aconitase[11] gave evidence for 3-Fe centers which, according to our opinion, should be closely related to the Fe_3S_7 unit of **5** if tetrahedral metal coordination is assumed. An alternative model for the 3-Fe center of Dg fd II based on a six-membered Fe_3S_3 ring in the chair conformation has been proposed,[10] each iron atom having two terminal coordination sites to couple with the protein or small exogenous ligands. However, a Fe_3S_3 ring in the chair (as well as in the boat) conformation with Fe···Fe distances of ca. 2.7 Å fits perfectly well with the Fe_4S_4 cubane cluster core. Assuming S–Fe–S valence angles in the range observed in tetrahedral FeS_4 coordination sites, it is hard to imagine that two terminal ligands can be added to each Fe of the Fe_3S_3 cycle without introducing severe ligand repulsions. These arguments make us believe that the $[Fe_3S(o\text{-}(SCH_2)_2C_6H_2Me_2)_3]^{2-}$ cluster[5a] with an Fe_3S_7 frame similar to that of **5** should be a structural model for the 3-Fe sites at least of Dg fd II and of beef heart aconitase.

With respect to the oxidation state of iron in these sites and the number of associated inorganic sulfur atoms, the $[Fe_3S_4]$ core portion of **5** (Fe(1), Fe(2), Fe(3), S(1), S(2), S(4), S(5) (see Figure 5)) completed by three thiolate ligands to give the tetrahedral metal coordination represented by **8** could be a structural as well as an electronic representation.

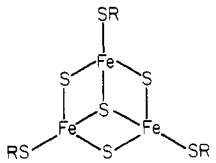

8

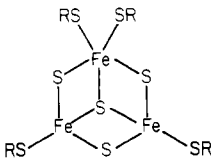

9

Another structural model that is derived from **8** by adding a second thiolate ligand to one of the three iron atoms resulting in the structure of **9** with a pentacoordinated metal site has the advantage of being completely compatible with mechanistic considerations concerning the reversible interconversion of 3-Fe and 4-Fe protein sites[11] and with the observed redox behavior.[12c]

In contrast to $[M_4S_4(SR)_4]^{n-}$ cubane clusters no iron members of the $[M_8S_6(SR)_8]^{n-}$ cluster family are yet known, though structural characteristics of their $[Fe_8S_6]^{n+}$ core are realized in several minerals such as bartonite.[27] A hypothetical iron cluster that is isoelectronic with $[Co_8S_6(SPh)_8]^{4-}$,[28] the only known example of this family, requires an oxidation state of +1, which has never been observed for iron in iron–sulfide–thiolate complexes. In fact, $[Fe_8S_6(SR)_8]^{n-}$ cluster anions comprising $Fe^{2+/3+}$ should be more realistic models, their synthesis being one of the subjects of our current interest in iron–sulfide–thiolate chemistry.

Though protein centers containing the $[Fe_8S_6]^{n+}$ core are not yet known, mixed-metal derivatives of the $[Fe_7MoS_6]^{m+}$

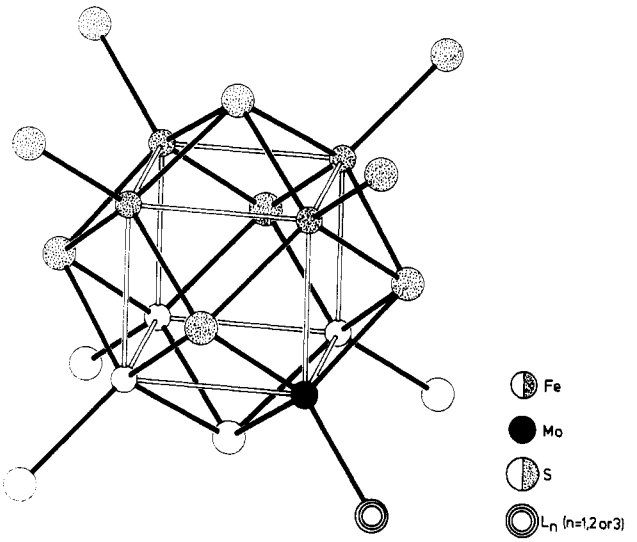

Figure 5. The $Fe_7MoS_{13}L_n$ frame of the $[Fe_7MoS_6(SR)_7L_n]^{z-}$ cluster (n = 1, 2, or 3) proposed as a model for the Mo–Fe center of nitrogenase. The dotted atoms indicate the Fe_4S_9 unit observed in the $[Fe_6S_9(SCH_2Ph)_2]^{4-}$ anion of **1**.

type match the requirements of both Fe and Mo sites in the Mo–Fe cofactor of nitrogenase with respect to their metal and inorganic sulfur environments as deduced from EXAFS data.[29]

A possible structural model of the Fe–Mo center of nitrogenase based on the $[Fe_7MoS_6]^{m+}$ cluster core has been derived by Holm et al.[28] from the architecture of the $[Co_8S_6(SPh)_8]^{4-}$ cluster and independently by Henkel et al.[6b] from the structural principles of the $[Fe_4S_9]$ core portion of **5**. This core portion is depicted as a fraction of the hypothetical $[Fe_7MoS_6(SR)_7L_n]^{z-}$ cluster anion (**10**) shown in Figure 5. The $[Fe_6S_6]^{4+}$ core of the recently prepared $[Fe_6S_6I_6]^{2-}$ cluster anion[30] is derived from the $[Fe_7MoS_6]^{m+}$ core by removal of the Mo atom and the opposite iron atom from the metal cube and thus represents another fraction of **10**. According to Figure 5, each Fe atom has one potential coupling site to the protein chain, probably occupied by a cysteinyl S atom, whereas the number of additional ligands (not necessarily S) completing the coordination of Mo may be one, two, or three.

In the light of our present knowledge concerning structural and compositional features of the Mo–Fe centers of nitrogenase,[29] the $[Fe_7MoS_6(SR)_7L_n]^{z-}$ cluster does not suffer from substantial inconsistencies as do all other models proposed in the literature.[31,32]

The $[(Fe_6S_9(SMe)_2)_2Na_2]^{6-}$ anion of **3** can be regarded as a mixed-metal–sulfur cluster with sodium atoms occupying coordination sites similar to those of transition-metal atoms. In contrast to transition-metal–sulfur interactions the sodium–sulfur contacts have to be considered to be predominantly electrostatic in origin so that the occurrence of such clusters is probably restricted to the solid state. The architecture of this anion can be described in terms of $[Fe_3NaS_4(SR)_6]^{5-}$ cubane units that are condensed via adjacent sodium and sulfur corners to form the tetrameric sodium–iron–sulfur cluster

(26) Henkel, G.; Tremel, W.; Krebs, B. *Angew. Chem.* **1983**, *95*, 317; *Angew. Chem., Suppl.* **1983**, 323; *Angew. Chem., Int. Ed. Engl.* **1983**, *22*, 319.
(27) Evans, H. T., Jr.; Clark, J. R. *Am. Mineral.* **1981**, *66*, 376.
(28) (a) Holm, R. H. *Chem. Soc. Rev.* **1981**, *10*, 455. (b) Christou, G.; Hagen, K. S.; Holm, R. H. *J. Am. Chem. Soc.* **1982**, *104*, 1744.
(29) (a) Cramer, S. P.; Gillum, W. O.; Hodgson, K. O.; Mortenson, L. E.; Stiefel, E. I.; Chisnell, J. R.; Brill, W. J.; Shah, V. K. *J. Am. Chem. Soc.* **1978**, *100*, 3814. (b) Antonio, M. R.; Teo, B.-K.; Orme-Johnson, W. H.; Nelson, M. G.; Groh, S. E.; Lindahl, P. A.; Kanzlarich, S. M.; Averill, B. A. *J. Am. Chem. Soc.* **1982**, *104*, 4703.
(30) Saak, W.; Henkel, G.; Pohl, S. *Angew. Chem.* **1984**, *96*, 153; *Angew. Chem., Int. Ed. Engl.* **1984**, *23*, 150.
(31) Averill, B. A. *Struct. Bonding (Berlin)* **1983**, *53*, 59.
(32) Teo, B. K. In "EXAFS Spectroscopy—Techniques and Applications"; Teo, B. K., Joy, D. C., Eds.; Plenum Press: New York, 1981; Chapter 3.

Table VI. Summary of Averaged S-Fe Bond Lengths and Distances from the Unweighted Least-Squares Planes Defined by the Fe_6 Frameworks for the Anions $[Fe_6S_9(SCH_2Ph)_2]^{4-}$ (I), $[(Fe_6S_9(SMe)_2)_2Na_2]^{6-}$ (II), $[Fe_6S_9(S\text{-}t\text{-}Bu)_2]^{4-}$ (III), and $[Fe_6S_9(SEt)_2]^{4-}$ (IV)

	I	II	III	IV
		S-Fe Bond Lengths (Å)[a]		
S^t-Fe^b	2.283 (2×)	2.273	2.268 (2×)	2.287 (2×)
(μ-S^b)-Fe^b	2.249 (4×)	2.258 (2×)	2.248 (4×)	2.249 (4×)
(μ-S^b)-Fe^a	2.215 (4×)	2.227 (2×)	2.211 (4×)	2.220 (4×)
(μ-S^a)-Fe^a	2.224 (4×)	2.207 (2×)	2.220 (4×)	2.232 (4×)
(μ_3-S)-Fe^b	2.259 (2×)	2.239	2.256 (2×)	2.267 (2×)
(μ_3-S)-Fe^a	2.313 (4×)	2.297 (2×)	2.297 (4×)	2.316 (4×)
(μ_4-S)-Fe^a	2.333 (4×)	2.347 (2×)	2.317 (4×)	2.340 (4×)
		Distances from the Best Planes (Å)[b]		
Fe(1)	−0.099	0.058	−0.135	−0.138
Fe(2)	0.037	−0.034	0.062	0.078
Fe(3)	0.083	−0.024	0.082	0.075
Fe(4)	0.007	−0.034	0.047	0.056
Fe(5)	0.047	−0.024	0.068	0.051
Fe(6)	−0.075	0.058	−0.124	−0.122
S(1)	−1.240	−1.336	−1.193	−1.221
S(2)	1.683	1.648	1.663	1.682
S(3)	1.654	1.648	1.644	1.661
S(4)	−1.137	−1.173	−1.248	−1.198
S(5)	−1.176	−1.151	−1.158	−1.141
S(6)	0.847	0.663	0.891	0.900
S(7)	0.904	0.663	0.893	0.907
S(8)	−1.081	−1.151	−1.184	−1.197
S(9)	−1.274	−1.173	−1.269	−1.166
S(10)	0.374	1.002	0.452	0.327
S(11)	0.648	1.002	0.357	0.500

[a] The indices for S and Fe are defined in the text. [b] The atomic numbering scheme refers to I (see Figure 1).

Table VII. UV/Visible and ^1H NMR Data of $[Fe_6S_9(SR)_2]^{4-}$ Clusters and Solid-State Infrared Absorptions of **1**-**3** in the Region of Fe-S Stretching Vibrations

R	λ_{max}, nm (ϵ_M, M^{-1} cm^{-1})[a]	$(\Delta H/H_0)^{iso}$, ppm[b]	IR bands, cm^{-1}
$CH_2C_6H_5$[c]	322 (35 900), 412 (26 600), ~535 (sh, 13 000)	CH_2,[d] −13.4 (CD_3CN), −13.0	395, 377, 366, 345, 322
C_2H_5[c]	321 (35 700), ~410 (25 700),[e] ~530 (sh, 13 000)	CH_2, −13.2; CH_3, −1.47	~392 (sh), ~378 (sh), 365, 333, 319, 294
CH_3[f]	320, ~410 (sh), ~530 (sh)	−15.45	403, 382, 373, 343, ~321 (sh), 297
$t\text{-}C_4H_9$[g]	319 (32 000), 412 (24 500), ~530 (sh, 12 000) (Me_2SO)	−1.5	
C_6H_5[g,h]	300 (40 000), ~350 (sh, 32 000), ~420 (sh, 25 200), ~530 (sh, 14 100) (Me_2SO)	o-H, +1.6; m-H, −0.97; p-H, +2.43	

[a] Acetonitrile solutions unless otherwise stated. [b] At 296 K; Me_2SO-d_6 solutions unless otherwise stated. [c] Et_4N^+ salt. [d] For ring proton shifts see text. [e] Broad absorption maximum. [f] UV/visible and NMR data, Ph_4P^+ salt; IR data, **3**. [g] $Me_3NCH_2Ph^+$ salt; data taken from ref 6d. [h] See ref 21.

$[(Fe_{3/1}Na_{1/2}S_{3/1}S_{1/2}(SMe)_{1/1})S_{2/2}]_4^{6-}$. As a consequence of the additional sodium centers the Fe–S bonds in **4** exhibit characteristic changes as compared to **5** though the overall architectures of their Fe_6S_9 units are quite similar as are the mean Fe–S bond lengths.

This is best reflected by comparison of corresponding Fe–S bond lengths, which are slightly elongated if S binds to Na but shortened if not. For comparison purposes a summary of comparable Fe–S bond lengths of **6**, **7**, and the $[Fe_6S_9(SCH_2Ph)_2]^{4-}$ anion of **1** together with corresponding values of the $[(Fe_6S_9(SMe)_2)_2Na_2]^{6-}$ anion of **3** is given in Table VI. This table also includes the distances of the Fe and S atoms from the best planes of the Fe_6 frames of **1**, **3**, **6**, and **7**.

The sodium atoms are located within trigonal prisms formed by opposite S_3 triangles of two symmetry-related Fe_6S_9 subunits. They complete the metal environment of S(1) toward a trigonal prism, each trigonal face being defined by two iron atoms and one sodium atom. Due to the long Na–S distances (mean value 2.960 Å) the geometry of the cubane-like Fe_3NaS_4 subunit of **3** differs considerably from the more regular one observed in exclusively iron-containing clusters, reflecting the different modes of metal–sulfur interactions in **3**.

From inspection of Table VI some minor differences in the structures of the $[Fe_6S_9(SR)_2]^{4-}$ anions of **1**, **6**, and **7** are obvious, which can be attributed to polarization effects in the crystal lattices.

Solubility Properties and Electronic Spectra. The compounds **1** and **2** are soluble in acetonitrile, DMF, and Me_2SO, while **3** is nearly insoluble in the first two solvents and only moderately soluble in Me_2SO. This different behavior of **3** is certainly due to the sodium ion in the crystal lattice and the small size of the methylthio ligand. As expected, the Ph_4P^+ salt of $[Fe_6S_9(SMe)_2]^{4-}$ shows a higher solubility in organic solvents than **3**, and therefore it was used in the determination of the anion properties in solution. The electronic spectra of the $[Fe_6S_9(SR)_2]^{4-}$ complexes (R = CH_2Ph,[33] Me, Et) between 300 and 700 nm in acetonitrile solution exhibit the same principal band shapes and relative band intensities as the spectrum of $[Fe_6S_9(S\text{-}t\text{-}Bu)_2]^{4-}$ in Me_2SO solution.[6d] The absorptions presumably originate in charge-transfer processes. Spectral data are given in Table VII. The UV–visible spectra of $[Fe_6S_9(SR)_2]^{4-}$ clusters differ from those of the corresponding $[Fe_4S_4(SR)_4]^{2-}$ complexes, especially in the presence of a shoulder at ca. 530–535 nm.[34] This shoulder, together with the two bands near 320 and 410 nm, should be useful for the identification of possible Fe_6S_9 centers in proteins, since known iron–sulfur centers (except the Fe_2S_2 ones) have no

(33) The absorptions given in a preliminary report[6b] are partially due to or effected by decomposition products.
(34) DePamphilis, B. V.; Averill, B. A.; Herskovitz, T.; Que, L., Jr.; Holm, R. H. *J. Am. Chem. Soc.* **1974**, *96*, 4159.

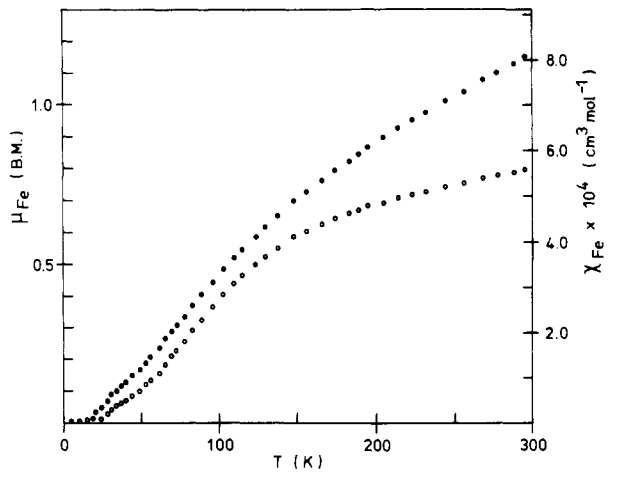

Figure 6. Temperature dependence of the magnetic moment (upper curve, left scale) and susceptibility (lower curve, right scale) per iron atom of $(Et_4N)_4[Fe_6S_9(SCH_2Ph)_2]\cdot H_2O$.

characteristic spectral features in the 500–600-nm region.[35,36] Under appropriate conditions protein Fe_2S_2 clusters can be identified by three absorption maxima below 500 nm (325–333, 410–425, and 455–470 nm in the oxidized form[2]).

A striking property of compounds **1–3** is their excellent water solubility. This seems to arise from the relatively high anion charge and the small proportion of hydrophobic groups, i.e. hydrocarbon residues, in the anions. The solutions in water are as brown as those in organic solvents. The principal features of the UV–visible spectra in acetonitrile solution are retained in aqueous solution. However, in the latter the absorption maxima are shifted to higher energies by ca. 7–20 nm and the band shapes are less pronounced, possibly indicating partial decomposition by hydrolysis.

Magnetic Properties. The temperature dependence of the magnetic susceptibility of **1** in the solid state was examined. A diamagnetic correction was applied, calculated to be $\chi_{dia} = -170 \times 10^{-6}$ cm^3 mol^{-1} per iron atom with the use of constants given by Haberditzl.[37] χ_{para}, plotted vs. T, revealed a minimum at 50–60 K. Below 20 K a Curie–Weiss law is obeyed, defined as $\chi_{para} = C/(T - \Theta)$ with $C = 0.0118$ cm^3 mol^{-1} K and $\Theta = -4.6$ K. These observations can be explained if traces of paramagnetic contaminations are present in the sample. Under this assumption the experimental values of χ_{para} were corrected, with contributions of mononuclear impurities taken into account. The final values of the magnetic moment μ_{Fe} and susceptibility χ_{Fe} per iron atom as a function of temperature are given in Figure 6.

The room-temperature value of 1.15 μ_B/iron atom is similar to those determined for $[Fe_6S_9(S\text{-}t\text{-}Bu)_2]^{4-}$ in solution (1.12 μ_B/Fe),[6d] $[Fe_4S_4(SR)_4]^{2-}$ (ca. 1.1 μ_B/Fe),[4b] and $[Fe_2S_2(SR)_4]^{2-}$ clusters (ca. 1.4 μ_B/Fe).[38] The magnetic susceptibility decreases with decreasing temperature and approaches zero at ca. 20 K, indicating a diamagnetic ground state below this temperature. This magnetic behavior is qualitatively consistent with antiferromagnetic exchange coupling of the iron atoms in the $[Fe_6S_9]^{2-}$ core. A theoretical fit of the magnetic susceptibility data of the hexanuclear cluster is in progress.[39]

Proton Magnetic Resonance Properties. It has been reported that the paramagnetism of $[Fe_6S_9(SR)_2]^{4-}$ clusters (R = *t*-Bu, Ph, Et) causes isotropic shifts of thiolato ligand ^{1}H NMR signals that are similar to, but distinguishable from, those of $[Fe_4S_4(SR)_4]^{2-}$ clusters.[6d,40] Proton isotropic shifts $(\Delta H/H_0)^{iso}$ of the hexanuclear complexes are given in Table VII. For their evaluation the free mercaptans were used as diamagnetic reference substances. Mercaptan proton resonances were taken from ref 40, except those of methyl and benzyl mercaptan in Me_2SO-d_6, for which −1.97 ppm (d) and −3.73 ppm (CH_2, d), respectively, were measured. As in the case of $[Fe_4S_4(SCH_2Ph)_4]^{2-}$[40] the ring proton shifts of $[Fe_6S_9(SCH_2Ph)_2]^{4-}$ are small, but exact signal positions could not be resolved. Compared with the $[Fe_4S_4(SR)_4]^{2-}$ dianions, the S-CH_2 downfield shifts of the hexanuclear clusters are 20–35% larger. On the other hand, the S-CH_2 shift of the $[Fe_4S_4(SCH_2Ph)_4]^{3-}$[41] trianion is ca. 2.3 times as large as that of $[Fe_6S_9(SCH_2Ph)_2]^{4-}$. This sequence corresponds qualitatively with the considerably higher magnetic moment per iron atom of the trianion (2.57 *vs.* 1.15 μ_B for the hexanuclear cluster and 1.07 μ_B for the tetrameric dianion (Et_4N^+ salts, solid-state room-temperature values)).[4b]

Table VIII. Average Formal Oxidation States of Iron and β Values[a] for Fe/S/SR Clusters

cluster type	Ox_{Fe}	β (z = 2.5)
$[Fe_2S_2(SR)_4]^{2-}$	+3.00	4.50
$[Fe_3S(SR)_6]^{2-}$	+2.00	2.83
$[Fe_3S_4(SR)_4]^{3-}$	+3.00	4.67
$[Fe_4S_4(SR)_4]^{2-}$	+2.50	3.50
$[Fe_6S_9(SR)_2]^{4-}$	+2.67	4.08

[a] See text.

As expected for paramagnetic species, the isotropically shifted signals of the $[Fe_6S_9(SR)_2]^{4-}$ complexes are broadened.[42] Protons attached to α-carbon atoms have signals with typical half-intensity widths of 100–200 Hz. Usually, Me_2SO-d_6 solutions containing $[Fe_6S_9(SR)_2]^{4-}$ complexes (R = Me, Et, CH_2Ph) were ca. 0.01–0.02 M, and the shifts were found nearly independent of concentration. The SCH_2 signal of **1** in a concentrated Me_2SO-d_6 solution is shifted downfield by ca. 0.3 ppm compared with its position at concentrations in the range mentioned above; moreover, all signals are extremely broadened. At lower concentrations the Me_4Si and solvent signals are sharp whereas those of the Et_4N^+ cations are still broader than in the spectra of diamagnetic Et_4N^+ salts. This seems to indicate some association of cations and paramagnetic anions.

In the range 225–340 K a linear relationship between $(\Delta H/H_0)^{iso}$ and the temperature T is found for the SCH_2 protons of **1** in CH_3CN, to be expressed by

$$(\Delta H/H_0)^{iso} = (-10.31 \times 10^{-3})T - 10.34 \text{ ppm}$$

Between 196 and 296 K the $\chi_{Fe}(T)$ curve is also linear, and χ_{Fe} is given by

$$\chi_{Fe} = (7.94 \times 10^{-7})T + 3.25 \times 10^{-4} \text{ cm}^3 \text{ mol}^{-1}$$

The absolute values of $(\Delta H/H_0)^{iso}$ and χ_{Fe} both increase with increasing temperature.

It has been demonstrated for the $[Fe_4S_4(SCH_2Ph)_4]^{2-,3-}$ clusters that the observed isotropic shifts are mainly of contact origin, i.e. $(\Delta H/H_0)^{iso} \simeq (\Delta H/H_0)^{con}$.[40,41] Considering the similarities between these complexes and $[Fe_6S_9(SCH_2Ph)_2]^{4-}$, as reflected by their spectral and magnetic properties, it seems

(35) Moura, I.; Moura, J. J. G. In "The Biological Chemistry of Iron"; Dunford, H. B., Dolphin, D., Raymond, K. N., Sieker, L., Eds.; Reidel: Dordrecht, The Netherlands, 1982; Section E.
(36) Orme-Johnson, W. H.; Orme-Johnson, N. R. In "Iron-Sulfur Proteins"; Spiro, T. G., Ed.; Wiley: New York, 1982; Chapter 2.
(37) See ref 20, Chapter 4.
(38) Gillum, W. O.; Frankel, R. B.; Foner, S.; Holm, R. H. *Inorg. Chem.* **1976**, *15*, 1095.
(39) Lueken, H., private communication.
(40) Holm, R. H.; Phillips, W. D.; Averill, B. A.; Mayerle, J. J.; Herskovitz, T. *J. Am. Chem. Soc.* **1974**, *96*, 2109.
(41) Reynolds, J. G.; Laskowski, E. J.; Holm, R. H. *J. Am. Chem. Soc.* **1978**, *100*, 5315.
(42) Swift, T. J. In "NMR of Paramagnetic Molecules"; La Mar, G. N., Horrocks, W. D., Jr., Holm, R. H., Eds.; Academic Press: New York, 1973; Chapter 2.

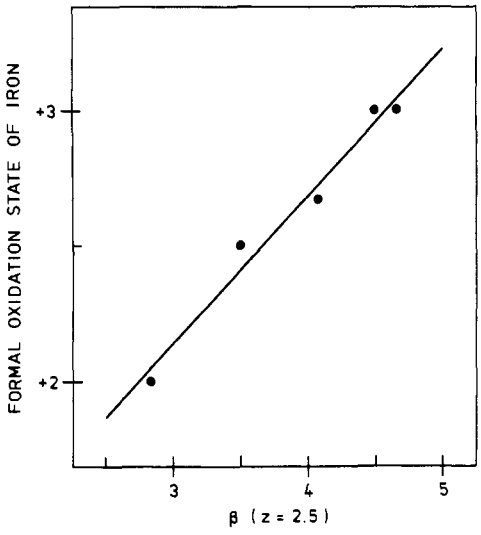

Figure 7. Relationship between the formal oxidation state of iron in Fe/S/SR clusters and β for $z = 2.5$ (see text). The plotted values are taken from Table VIII.

probable that contact interactions are dominating in the hexanuclear cluster as well.

Empirical Correlation between Composition and Formal Oxidation State of Iron for Fe–S–SR Clusters. In Table VIII all hitherto known types of iron–sulfide–thiolate clusters are given. They meet the following conditions: (i) The iron atoms are tetrahedrally coordinated by sulfur. (ii) The clusters form spontaneously in the reaction of (a) $FeCl_3$ (or $FeCl_2$) and RS^- or (b) Fe(II) thiolate complexes with inorganic sulfur compounds (S^{2-}, S_x^{2-}, and S_8). (iii) The reaction medium is methanol, with the only exception of $[Fe_3S_4(SR)_4]^{3-}$ complexes, which could be isolated from acetonitrile and acetone solutions, respectively.[6e,7]

In order to demonstrate a trend between composition and formal oxidation state for these clusters, we define a ratio, α (eq 2), where N_{Fe}, N_{RS}, and N_S are the number of iron, coordinating thiolate sulfur, and inorganic sulfur atoms, respectively. α increases with increasing number of iron atoms

$$\alpha = N_{Fe}/(N_{RS} + N_S) \quad (2)$$

and seems to approach a limiting range for large N_{Fe} values. This follows qualitatively from a progressive connection of FeS_4 tetrahedra.

A modified form of eq 2 is obtained by introducing the parameter z, which allows weighting of the two types of ligands (eq 3).

$$\beta = (N_{RS} + zN_S)/N_{Fe} \quad (3)$$

The meaning of eq 3 is that a nearly linear relationship between the formal oxidation state of iron (Ox_{Fe}) and β results if a z value of 2.5 is chosen. This relationship is given in Figure 7. The fitted straight line defined by $Ox_{Fe} = 0.54\beta + 0.51$ can be interpreted as a stability curve of Fe/S/SR clusters for which above-mentioned conditions i–iii are valid. The Ox_{Fe} vs. β points for the reduced and oxidized forms of the clusters given in Table VIII are located below and above this stability curve, respectively.

An interpretation of z can be given by comparison of the data for $[Fe_3S(SR)_6]^{2-}$ and $[Fe_3S_4(SR)_4]^{3-}$. Both clusters contain the same number of iron atoms, and according to the relation between N_{Fe} and α (see above), their $N_{RS} + N_S$ values are similar. Due to the low oxidation state of iron in $[Fe_3S(SR)_6]^{2-}$ the value of β (and $N_{RS} + 2.5N_S$) is small (cf. eq 3), and the N_S/N_{RS} ratio must be smaller than for the second cluster, which contains iron in a higher oxidation state. Thus the factor $z = 2.5$ probably reflects the stronger stabilizing effect of S^{2-} toward higher oxidation states of iron compared with that of RS^-.

Though the correlation shown in Figure 7 is of limited statistical significance due to the small number of empirical data, it demonstrates an obvious tendency that could be used to predict the most probable oxidation state of iron under conditions i–iii for a given structural type of Fe/S/SR cluster. For example: (a) $[Fe_3S_3(SR)_6]^{n-}$ complexes should be structural analogues for the 3-Fe site of *A. vinelandii* ferredoxin I. The β value of these complexes is 4.50, and thus the predicted value of Ox_{Fe} is +2.94, which seems reasonable considering the oxidation states of iron in the trinuclear protein center.[43] (b) For the $[Fe_8(\mu_4\text{-}S)_6(SR)_8]^{n-}$ cluster type the β value is 2.88. The predicted oxidation state of iron is +2.06. An analogous Co(II) complex, $[Co_8(\mu_4\text{-}S)_6(SPh)_8]^{4-}$, has been described.[28]

Acknowledgment. Financial support from the Minister für Wissenschaft und Forschung des Landes Nordrhein-Westfalen and from the Fonds der Chemischen Industrie is gratefully acknowledged. H.S. wishes to thank the Stiftung Stipendien-Fonds des Verbandes der Chemischen Industrie for the award of a predoctoral fellowship. We also thank Dr. H. Lueken for performing the magnetic measurements and M. Dartmann, M. Pützler, and D. Kaiser for technical assistance.

Registry No. 1, 82616-29-3; 2, 85585-66-6; 3, 90065-79-5; Fe, 7439-89-6.

Supplementary Material Available: FT IR spectra of polycrystalline 1–3 (Figure S-1) and observed and calculated structure factors for 1 and 3 (Tables S-I and S-II), thermal parameters for 1 and 3 (Tables S-III and S-IV), interatomic distances and angles involving carbon for 1 and 3 (Tables S-V and S-VI), and positional parameters of the hydrogen atoms for 1 (Table S-VII) (61 pages). Ordering information is given on any current masthead page.

(43) Emptage, M. H.; Kent, T. A.; Huynh, B. H.; Rawlings, J.; Orme-Johnson, W. H.; Münck, E. *J. Biol. Chem.* **1980**, *255*, 1793.